PUBLICATION NO. 52 1/2015

NORDIC CONCRETE RESEARCH

EDITED BY
THE NORDIC CONCRETE FEDERATION

CONCRETE ASSOCIATIONS OF: DENMARK
FINLAND
ICELAND
NORWAY
SWEDEN

PUBLISHER: NORSK BETONGFORENING
POSTBOKS 2312, SOLLI
N - 0201 OSLO
NORWAY

VODSKOV, JUNE 2015

Pb^{2+} Adsorption by Calcium Silicate Hydrate Synthesized from Steel Slag

Shuping Wang
M.Eng., Ph.D.
Division of Building Technology, Chalmers University of Technology, SE- 412 96, Gothenburg
College of Material Science and Engineering, Chongqing University, CN-400045, Chongqing
E-Mail: shuping@chalmers.se

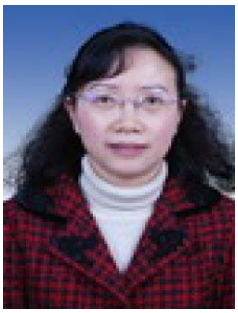

Xiaoqin Peng
Ph.D., Prof.
College of Material Science and Engineering, Chongqing University, CN-400045, Chongqing
E-Mail: pxq01@cqu.edu.cn

Mei Li
M. Eng.
College of Material Science and Engineering, Chongqing University, CN-400045, Chongqing
E-Mail: 674842676@qq.com

Luping Tang
Ph.D., Prof.
Division of Building Technology, Chalmers University of Technology, SE- 412 96, Gothenburg
E-Mail: tang.luping@chalmers.se

ABSTRACT

This study aims to investigate the adsorption properties of Pb^{2+} by calcium silicate hydrate synthesized from steel slag. The influence of various factors on the adsorption properties was investigated. The static desorption test was conducted to investigate the leaching of Pb^{2+}. The kinetic model and isotherm model of adsorption are then discussed. Results show that Pb^{2+} adsorption capacity of C-S-H depends on Ca/Si ratios. Kinetic adsorption data is in consistence with Lagergren pseudo-second-order model, and steady-state data fits to Langmuir isothermal model. Leaching result demonstrates that Pb^{2+} ions are stably adsorbed by C-S-H structures.

Key words: Pb^{2+} adsorption, calcium silicate hydrates, steel slag, adsorption model.

1. INTRODUCTION

Recently, solidification/stabilization technology (S/S) of cement-based material is widely studied on treating the heavy metal pollution and water treatment [1-5]. It is attributed to calcium silicate hydrate (C-S-H, C=CaO, S=SiO_2, H=H_2O), the main hydration product of cement paste. The main structures of C-S-H (Ca/Si molar ratio from 0.6 to 2) are disordered forms of 1.4 nm tobermorite and jennite, with a large specific surface area, high porosity and active sites such as hydroxyl groups [6,7]. Calcium silicate hydrates exhibit a large number of structural sites available for cation and anion binding [8]. Therefore, C-S-H structure plays an essential role in adsorption of heavy metals. The mechanism includes ion-exchange, adsorption and chemical trapping. Heavy metals such as Nd(III), Zn(II), Cd(II), Cr(IV) , U(IV) and Sr(II) adsorbed by C-S-H have been studied by many researchers [9-14]. The results show that the heavy metals are incorporated into the Ca-O sheets, absorbed in the interlayer of C-S-H, or ion-exchange with Ca^{2+} as the curing age increases.

Apart from cement hydration, C-S-H can also be obtained from waste slags, such as steel slag, which has a large amount of emission but low utilisation especially in China [15]. Wang et al. synthesized 11.3 Å tobermorite structures from steel slag by hydrothermal treatment [16]. Kuwahara and co-workers [17] reported that C-S-H prepared from the waste slag had good adsorption properties for removal of Cu^{2+}, phosphate ions and model protein diluted in water. Therefore, synthesized C-S-H is considered as a candidate for water purification on the heavy metals.

Lead (Pb), harmful to the health of human beings, is one of the main contaminations around the world; hence, how to treat it has become widely discussed. Xonotlite secondary particles were used to treat lead-bearing wastewater by Han, et al. [18], which indicated high Pb^{2+} removal. Investigations of Lee [19], Pierrard, Rimbault, and Aplincourt [20] suggested that Pb^{2+} fixed by C-S-H was affected by pH value of its pore solution. The main formation of Pb was $Pb_4SO_4(CO_3)_2(OH)_2$ and $3PbCO_3 \cdot 2Pb(OH)_2 \cdot H_2O$ at short time curing. The lead was adsorbed on the silica-rich surface to form C-Pb-S-H after long time cured together with acid attack. Pb^{2+} adsorbed by 1.1 nm tobermorite was also studied by Coleman, Trice, and Nicholson [21], indicating that the sorption conforms to the pseudo-second-order model and the uptake was up to 467 mg g^{-1} after 168-hour curing. However, the adsorption properties and mechanisms of lead on C-S-H are still poorly understood. In particular, there is seldom investigation on lead uptake in mild acidic medium.

This study explores the possibility of Pb^{2+} adsorption on calcium silicate hydrates synthesized from steel slag in mild acidic solutions. The influence of various factors, e.g. the properties and amount of C-S-H powder, adsorption time, Pb^{2+} concentrations, and pH values of the solution, on the adsorption properties are investigated. Furthermore, the kinetic and isotherm behaviours of adsorption by C-S-H are discussed.

2. EXPERIMENTAL

2.1 Materials

The main chemical compositions of steel slag (Shougang Group, Beijing) used in this study are listed in Table 1. It was obvious that the steel slag consisted of CaO, SiO_2, MgO, Al_2O_3, and Fe_2O_3, with Ca/Si molar ratio of 2.17. The specific surface area measured by Blaine Air

Permeability was 474 m^2 kg^{-1}. The main mineral phases in this steel slag were C_3S and C_2S according to XRD analysis. There is no doubt that the slag was available for synthesizing calcium silicate hydrate.

Table 1 – Main chemical composition of steel slag

Components	CaO	SiO_2	Fe_2O_3	Al_2O_3	MgO	P_2O_5
Content (%)	42.80	21.14	5.74	5.86	9.58	0.58

2.2 C-S-H synthesis

Calcium silicate hydrate powder was synthesized in an autoclave (Weihai Chemical Machinery Co. Ltd). Steel slag was mixed with lime (87.9% CaO) and quartz (99.09% SiO_2) at the Ca/Si molar ratio between 0.8 and 1.5. The mixture was cured at temperatures ranging from 150℃ to 185℃, for 7 hours, with the water to solid ratio (w/s, in mass) of 6, filtered and oven- dried at 80 ℃. The details of hydrothermal synthesis are in Table 2.

Table 2 – the hydrothermal synthesis of calcium silicate hydrates

index	Raw materials (%)			Ca/Si	w/s	Curing temperature (℃)	Curing time (h)
	Steel slag	quartz	lime				
A	70	20.00	10.00	1.2	6	150	7
B	70	20.00	10.00	1.2	6	185	7
C	70	14.19	15.81	1.5	6	150	7
D	80.28	19.72	0	1.5	6	185	7
E	70	27.96	2.04	0.8	6	185	7

2.3 Adsorption of Pb^{2+} by C-S-H

Pb^{2+} solutions were prepared by dissolving lead acetate (research grade, Jinshan Chemical Reagent Co., Ltd., Chengdu) in distilled water. 100mL solution was added in the beaker with a proper amount of C-S-H powder, adjusting the pH value of the solution to 2 to 7, stirring (100 rpm). These tests were all carried out at the room temperature. The concentration of Pb^{2+} after adsorption was measured, and influences of the powder amount, adsorption time, pH of solution, initial Pb^{2+} concentrations on C-S-H capacity were discussed. The removal ratio(R) and adsorption capacity (q) of Pb^{2+} by C-S-H were calculated as followed formulas:

$$R(\%) = {100\% \times (C_0 - C)}/{C_0} \quad (1)$$

$$q = {(C_0 - C) \times V}/{m_p} \quad (2)$$

Where C_0 is the initial concentration of Pb^{2+} (in mg L^{-1}); C indicates Pb^{2+} concentration after adsorption (in mg L^{-1}); V represents volume of solution (in L); m_p is the mass of hydrated calcium silicate powder (in g); and q is the amount of Pb^{2+} adsorbed by per unit C-S-H (in mg g^{-1})

2.4 Desorption test

To investigate the leaching of lead after having been adsorbed by C-S-H, static desorption measurement was carried out at room temperature. 1.5 gram powder with Pb^{2+} after equilibrium adsorbed was added into 100 ml distilled water or acetic acid solution (pH value of 5), respectively. After stirring (100 rpm) for 75 minutes, the solution was filtered and Pb2+ concentration of the solution was measured. The desorption ratio (ε) is calculated as following formula:

$$\varepsilon(\%) = \frac{C_1 V_1}{(C_0 - C)V} \times 100\% \quad (3)$$

C_0, C and V are described in the above section, where C_1 and V_1 represent the Pb^{2+} concentration and volume of the solution after desorption, respectively.

2.5 Product characterisation

XRD was applied to identify the crystalline phases of the synthesized C-S-H powders. The samples were detected by a Rigaku D/max-1200 X-ray powder diffraction apparatus (Cu Kα radiation), at a step size of 0.02^o with scanning rate of 2^o min^{-1}, and a scan range from 5^o to 70^o 2θ. SEM (scanning electron microscope Morphology, TESCAN VEGA II) with a voltage of 20KV and magnitude of 4~100,000 X was also employed for detecting the morphology of the hydrothermal products. FTIR spectroscopy (Nicolet5DXC) equipped with a KBr beam splitter was used for functional group analysis, with scanning wavenumber from 4000 to 400 cm^{-1}.

Pb^{2+} concentrations were measured via spectrometric atomic absorption apparatus (Hitachi Z-8000), at a wavelength of 283 nm, according to the standard of GB/T 9723-2007 (General rule for flame atomic absorption spectrometric analysis). The measurement was calibrated by measuring the absorbance at Pb concentrations of 0, 1, 2, 4, 6, 8, and 12 mg L^{-1}. Background was removed during analysis.

2.6 Adsorption models

Kinetic models

The Lagergren pseudo-first-order rate model and pseudo-second-order rate expression are used to study the adsorption kinetic model of Pb^{2+} by calcium silicate hydrates. These models describe adsorption of a solute by a solid surface, and adsorption processes in which the reaction rate is proportional to square [21-23].

The pseudo-first-order rate model can be expressed as following:

$$q^e = \frac{V(C_0 - C_e)}{m_p} \quad (4)$$

$$\log(q^e - q_t) = \log q^e - \frac{k_1}{2.303} t \quad (5)$$

Where q^e(in mg·g^{-1}) is the extent of sorption at equilibrium according to equation (2), C_e (in mg·L^{-1}) is the steady-state concentration of the metal ion in solution, q_t (in mg·g^{-1}) is the extent of adsorption at time *t*, and k_1(in min^{-1}) is the apparent pseudo-first-order rate constant of adsorption.

The expression of pseudo-second-order rate is:

$$\frac{t}{q_t} = \frac{1}{k_2 (q^e)^2} + \frac{1}{q^e} t \tag{6}$$

Where k_2 is the apparent pseudo-second-order rate constant of adsorption (in g mg^{-1} min^{-1}). If there is a linear plot of t/q_t against *t*, pseudo-second-order rate equation is satisfied.

Isothermal models

Adsorption isothermal equation reflects the relation between adsorptive capacity and the concentration of solution under a fixed temperature. There are mainly two models. One is Langmuir isotherm model reflecting the monolayer adsorption onto solid surfaces, and the other is Freundlich isothermal model which is also widely applied in liquid-solid adsorption system.

The linear form of the Langmuir isothermal model, used to illustrate uptake of metal ions from solution by a solid substance, can be described as follows [22, 23]:

$$\frac{C_e}{q^e} = \frac{1}{q_m b} + \frac{C_e}{q_m} \tag{7}$$

In equation (7) q_m is the maximum adsorptive capacity (in mg·g^{-1}) and *b* is the Langmuir constant (in L·mg^{-1}). Other parameters are described as above. q_m, and *b* is estimated from the intercept and the slop of the plot of C_e/n_s against C_e.

Freundlich isothermal model is described as:

$$\log q^e = \log K + \frac{1}{n} (\log C_e) \tag{8}$$

Where *K* is Freundlich constant and *1/n* is constant as well. This model is based on the assumption that the enthalpy of sorption becomes less negative [22].

3. ADSORPTION MODELS

3.1 Microstructures of synthesized C-S-H

XRD analysis

The XRD patterns of the synthetic samples are shown in Figure 1. Poorly crystalline C-S-H formed in all the samples due to the only appearance of diffraction peaks with the d-spacing of 0.302 nm (2θ 29º), 0.182 nm (2θ 18º) and 0.280 nm (2θ 32º) [7]. However, the final hydration phases were influenced by the hydrothermal curing process, such as the addition of lime, and the different Ca/Si molar ratios. Powder A and B consisted of C-S-H, and semi- tobermorite (d-spacing of 3.08 Å, 2.98 Å and 1.84Å) [16]. It is also found that SiO_2 was still present in Powder

A because of the appearance of intensive diffraction peak at 3.34 Å. As the Ca/Si ratio increased to 1.5 in Powder C, the dominant phase was poorly crystallized C-S-H. Besides, a zeolite- like gel was also generated due to the appearance of the peak at 3.17 Å. This phase is beneficial to the heavy metal incorporation. The main phase of Powder E was disordered C-S-H. In additional quartz was not completely consumed.

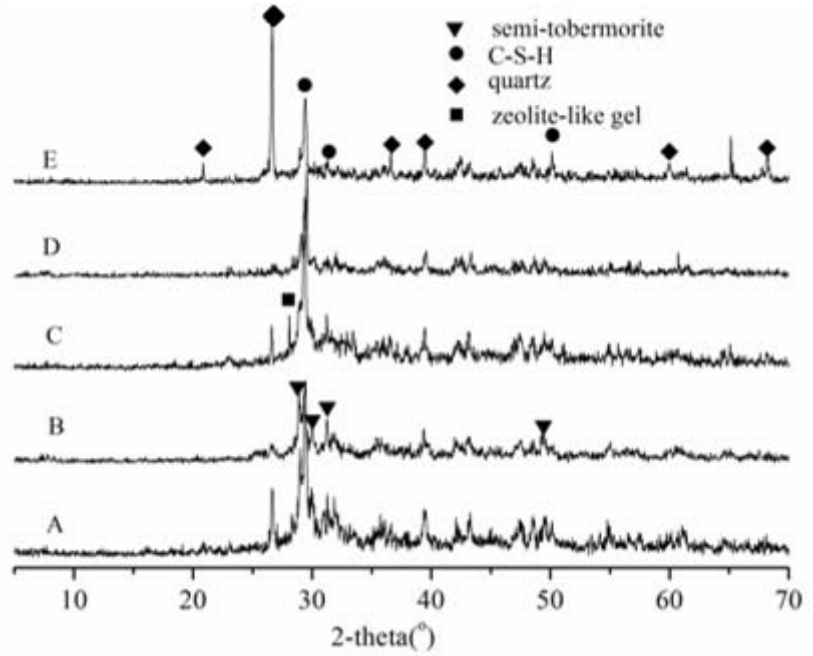

Figure 1 – XRD patterns of C-S-H samples made from steel slag by weight at the water/solid ratio of 6 and curing for 7 hours. The details for hydrothermal synthesis are shown in Table 2.

SEM analysis

The morphology of the synthetic C-S-H samples was investigated with SEM microscope (Figure 2). The powder particles showed non-crystallized structures, and were an aggregation of micro-scale morphology, which was 1 μm. It can be seen that the curing method, especially the Ca/Si molar ratio, affects the final morphology of the product . In sample A, which was prepared at 150 ℃ for 7 hours at the Ca/Si ratio of 1.2, foil or sheet-like structure appeared. When the Ca/Si ratio increased to 1.5, in sample C, C-S-H made up of fibril shaped grains with a loose reticular structure. It presented a porous surface, which is a so called as zeolite-like structure. In powder D, however, it exhibited a more compacted morphology with a lack of pronounced pores on the surface, which was attributed to the lack of lime addition.

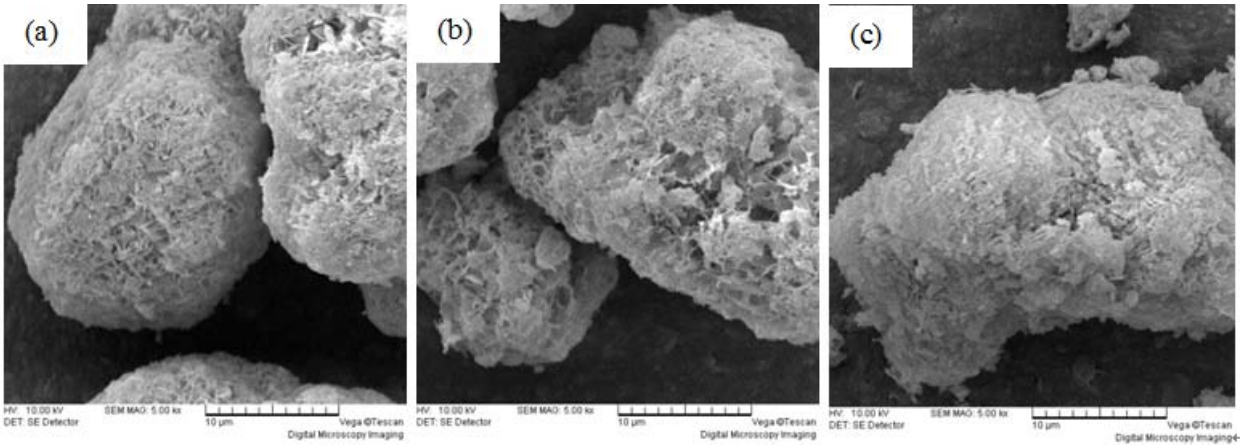

Figure 2 – SEM Photographs of the synthetic C-S-H:
(a) powder A synthesized from the mixture of 70wt% steel slag, 20wt% quartz and 10wt% lime with 1.2 Ca/Si molar ratio at 150 ℃ for 7 hours;
(b) Powder C synthesized from the mixture of 70wt% steel slag, 14.19wt% and 15.81wt% lime, with the Ca/Si molar ratio of 1.5 at 150 ℃ for 7h; and
(c) Powder D is corresponded to the product from 80.28wt% steel slag and 19.72wt% quartz without lime addition, the Ca/Si molar ratio of 1.5 at 185 ℃ for 7 hours

3.2 Pb^{2+} adsorption properties on C-S-H

The adsorption of Pb^{2+} by different C-S-H powders
C-S-H powders produced from different hydrothermal curing conditions were used to adsorb the Pb^{2+} with the concentration of 200 mg L^{-1}, and the results are shown in Figure 3. The adsorption properties were influenced by the synthesis process, generally on the Ca/Si molar ratio and the content of the lime. The sample C which was synthesized at 150 ℃ for 7 hours with the molar ratio of 1.5 presented the highest removal efficiency (about 99.67 %), and the adsorption capacity of Pb^{2+} was up to 19.53 mg g^{-1}. However, there were no satisfying results of Pb^{2+} adsorption by other types of powder, as the removal and adsorption capacity were lower than 90% and 18 mg g^{-1} respectively. The higher incorporation of Pb^{2+} in Powder C than other samples is attributed to its porous surface of the particles. In this case, Powder C was used for thermodynamic analysis on the subsequent adsorption study.

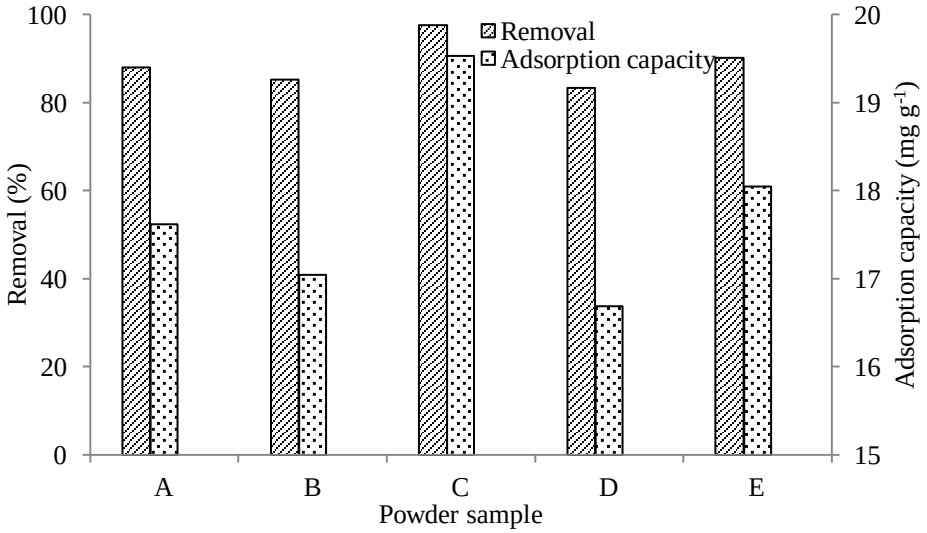

Figure 3 – Adsorption of Pb^{2+} by different kinds of C-S-H powders, synthesis of powder is in Table 2

Effect of C-S-H amount on Pb^{2+} adsorption

Different amount of calcium silicate hydrate powder were mixed with 100 mL Pb^{2+} solution (200 mg L^{-1}), adjusting the initial pH value of the mixture to 5. Adsorption time of 1 hour was applied. The result of adsorption is shown in Figure 4.

It can be seen that the removal efficiency increased rapidly from 31% to 96%, corresponding to the mass of C-S-H powder from 5 g L^{-1} to 15 g L^{-1}, followed by the stable adsorption efficiency. When 20 g L^{-1} of C-S-H powder was used, the removal of Pb^{2+} was up to 99%, with the residual concentration of Pb^{2+} solution 0.96 mg L^{-1}. Additionally, the adsorption capacity of Pb^{2+} by C-S-H was first increased and then declined as the amount of the powder increased. The maximum of adsorption capacity was 14.46 mg g^{-1} with the amount of 10 g L^{-1} powder, demonstrating that excessive amount of powder cannot be completely utilized. Therefore, in the following adsorption experiments, 15 g L^{-1} C-S-H powder is used.

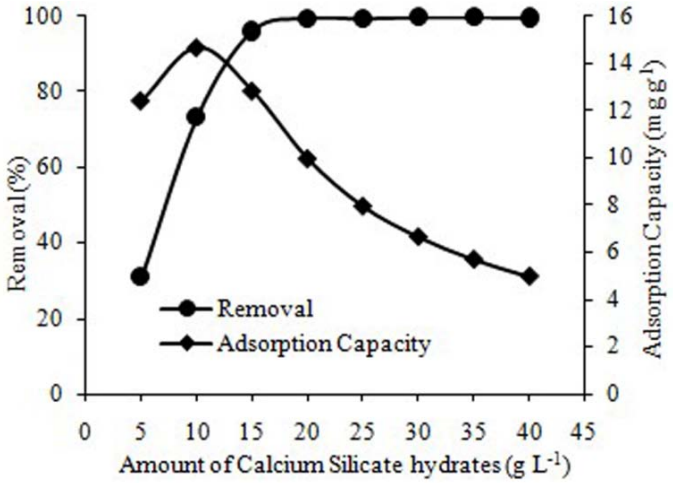

Figure 4 – Pb^{2+} removal at different amount of C-S-H powder

Effect of pH on Pb^{2+} adsorption

1.5 g calcium silicate hydration powder was mixed with 100 mL Pb^{2+} solution (Pb^{2+} concentration 200 mg L^{-1}). The initial pH values of the solution ranged from 2 to 7, with stirring

time of 1 hour (Figure 5). The removal efficiency and adsorption capacity of Pb^{2+} by C-S-H is influenced obviously by pH. At pH value of 2, the removal efficiency and adsorption capacity were only 11% and 1.52 mg g^{-1}, respectively. With pH increasing to 5, both the removal and adsorption capacity soared up to 96% and 12.73 mg g^{-1}, respectively. The data gradually increased when the pH value varied between 5 and 7. It is apparent that Pb^{2+} can be effectively adsorbed on C-S-H via weak acidic solution, since there are negative charges on the surface of C-S-H particles when pH of the solution is close to 7 [24]. On the other hand, the structure of C-S-H was damaged by strong acid solution, resulting in the poor adsorption.

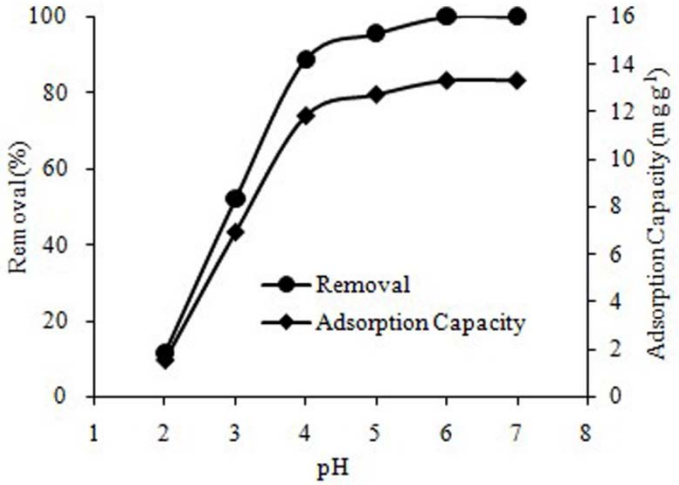

Figure 5 – Pb^{2+} adsorption in the solution of different pH values

Influence of stirring time on Pb^{2+} adsorption

Stirring time is another key factor on Pb^{2+} adsorption and reflects its equilibrium status. In this section, the adsorption properties of the duration from 30 minutes to 180 minutes were investigated (Figure 6). The curves indicated that the powder had an excellent adsorption property on Pb^{2+} even for only 30-minute reaction. The removal efficiency and the adsorption capacity were approximate 96% and 12.78 mg g^{-1}, respectively. Afterward, the removal efficiency increased to 99.4% and adsorption capacity of 13.25 mg g^{-1} at 75 minutes' adsorption. With stirring time extended, the values gradually improved, and residual Pb^{2+} concentration of the solution declined to 0.44 mg L^{-1} at 180 min, far below the emission standard of 1.0 mg L^{-1} (GB 8978-1988). According to Figure 6, the balance of adsorption was achieved after 75-minute adsorption.

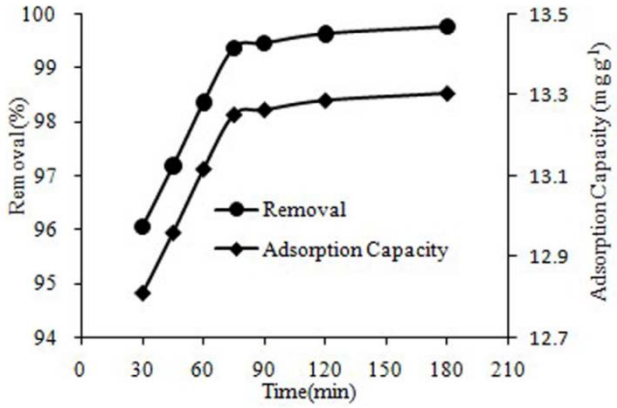

Figure 6 – Pb^{2+} adsorption properties at different stirring time

Influence of initial concentration of Pb^{2+} on adsorption

Herein, the results about adsorption of Pb^{2+} concentrations between 50 mg L^{-1} and 400 mg L^{-1} were discussed (Figure 7). With the increase of Pb^{2+} concentration from 50 mg L^{-1} to 400 mg L^{-1}, the adsorption capacity and Pb^{2+} concentration rapidly went up to 24.46 mg g^{-1} from 3.35 mg g^{-1}, which was attributed to the increase of contact sites between the calcium silicate hydrate powder and Pb^{2+}. On the contrary, the curve of removal appeared different tendency. It was stable at around 99% as the concentration ranged from 50 mg $L^{-1}$to 200 mg L^{-1}, and the maxium value was 99.4% at the Pb^{2+} concentration of 200 mg L^{-1}. The removal efficiency declined to 91.7% corresponding to the Pb^{2+} concentration of 400 mg L^{-1}.

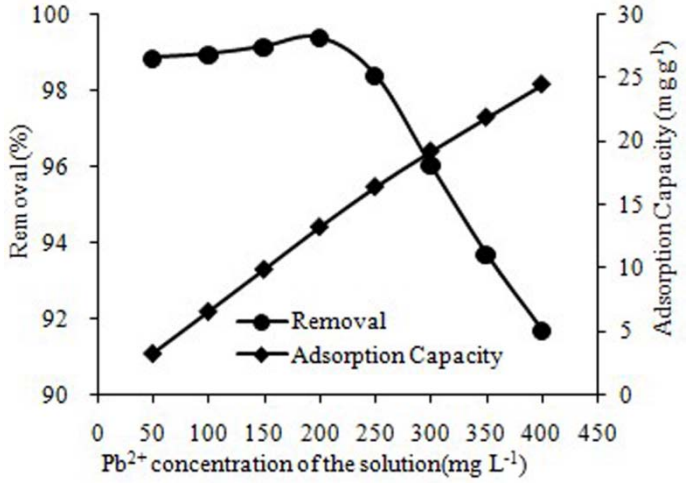

Figure 7 – adsorption properties with various Pb^{2+} concentration

3.3 Desorption of Pb^{2+} on C-S-H

Desorption tests were carried out both under distilled water and acidic solution, corresponding to the pH of 7.0 and 5.0. Results showed that the Pb^{2+} concentration was 0.16 mg L^{-1} after leaching experiment, indicating that the desorption ratio in water was as low as 0.08% according to equation (3). When acidic solution with pH of 5.0 was adopted, the leaching concentration of Pb^{2+} increased to 0.64 mL g^{-1}. It means that the desorption rate was 0.3%. The results demonstrate that Pb^{2+} can strongly adsorbed by C-S-H powder and leaching ratio in neutral solution is quite low, which might attribute to the combination between Pb^{2+} and functional groups.

4. ADSORPTION MODELS

4.1 Kinetic models

As mentioned previously, adsorption kinetic is analyzed by applying Lagergren pseudo-first-order model (equation (5)), and pseudo-second-order model (equation (6)). According to the data in Figure 6, the parameters of the two kinetic models are obtained (Figure 8, Table 3). The results show that higher correlation of the pseudo-second-order kinetic model (R^2 value of 1) than pseudo-first-order kinetic model (R^2 value of 0.96), demonstrating that the former affords a more appropriate description of the sorption process. Thus, the equilibrium adsorption q^e and constant rate k_2 are 13.09 mg g^{-1} and 7.82×10^{-2} g mg^{-1} min^{-1}, respectively. The kinetic results of

adsorption of metal cations by C-S-H powder is likely to reveal that the reaction is controlled by a number of transport and interaction process.

Table 3 – Statistical and kinetic datas of Pb^{2+} sorption on C-S-H

Lagergren (pseudo-first-order)			Lagergren(pseudo-second-order)		
q^e /(mg g^{-1})	$k_1 \times 10^{-2}$ /(min^{-1})	R^2	q^e /(mg g^{-1})	$k_2 \times 10^{-2}$ /(g mg^{-1} min^{-1})	R^2
13.30	6.86	0.96	13.09	7.82	1

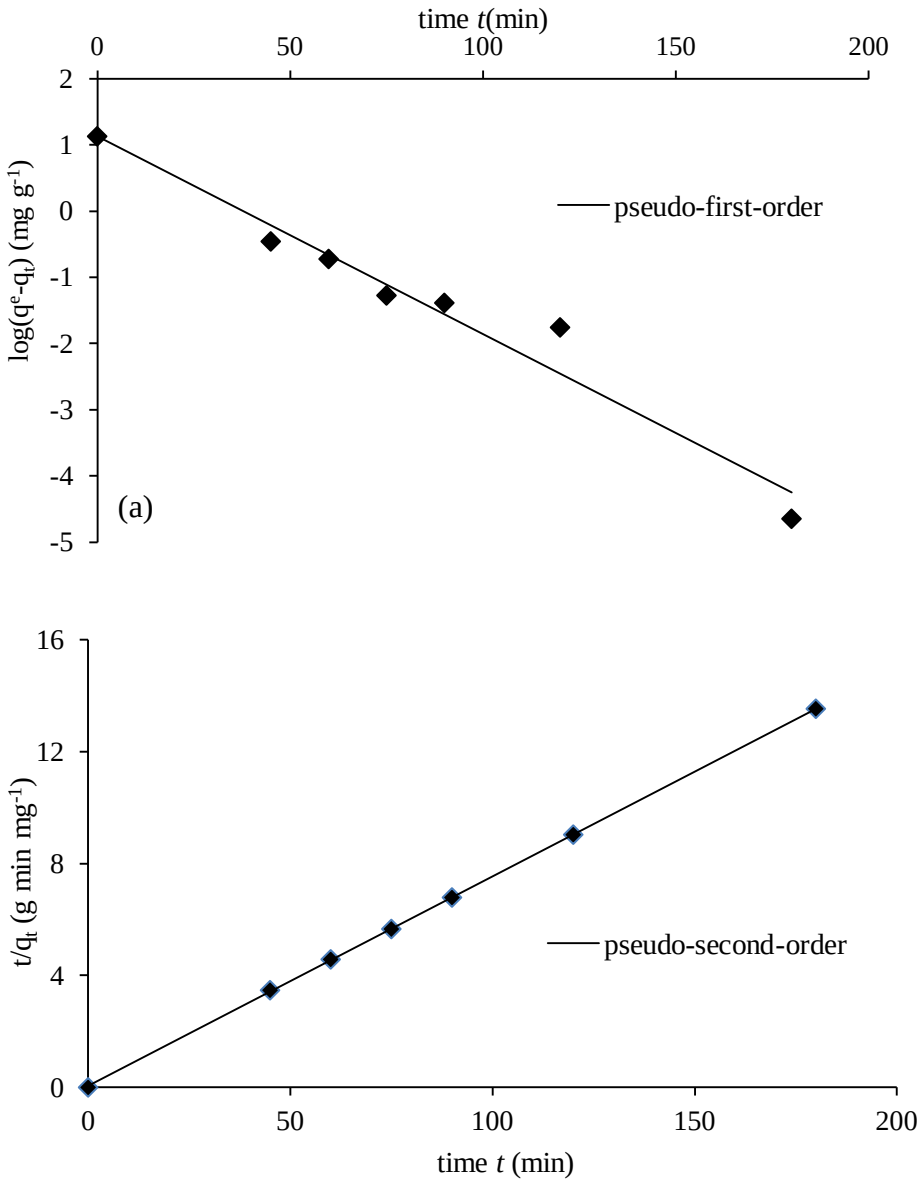

Figure 8 – kinetic model fitted to experimental data for the uptake of Pb^{2+} (a) pseudo-first-order model, and (b) pseudo-second-order model

Thus, adsorption rate is an important indicator to reflect the interaction between adsorbent and adsorbate. Generally, the adsorption processes include three stages [25], which are external-particle diffusion stage, intra-particle diffusion stage and adsorption-reaction stage. Weber-Morris equation (equation (9)) was used to describe the diffusion and transfer procedure of Pb^{2+} on C-S-H particle surface[26, 27]:

$$n_t^s = k_{id} t^{\frac{1}{2}} + b \quad (9)$$

Where b represents intercept, and k_{id} is intra-particle diffusion constant (in mg g^{-1} $min^{-1/2}$). In accordance with Figure 6, the adsorption rate tends to be constant after 75 minutes. By fitting the experiment data depending on the equation above, the correlation coefficiency R^2 is 0.92, an indication of linear relationship. As a result, it can be considered that before 75 minutes the adsorptive process is controlled by external-particle diffusion stage, followed by intra-particle procedure [28]. The value of k_{id} is 0.016 mg g^{-1} $min^{-1/2}$, and b of 13.10.

4.2 Isothermal models

In order to discribe the adsorption properties on the the surface of the powder, adsorption isothermal is studied. The adsorption isothermal curve obtained from Figure 7 is shown in Figure 9, which means the adsorption capacity of C-S-H on different Pb^{2+} equilibrium concentration. It can be inferred form equation (7) and (8) that the data are well correlated with the Langmuir isothermal model with R^2 of 0.99. While the Freundlich model is less appropriate for its R^2 of only 0.77 (Table 4). Thus, the adsorption conforms to monolayer adsorption and there are many active sites on the surface of C-S-H particles.

Table 4 – Langmuir and Freundlich isothermal parameters for the absorption of Pb^{2+} on C-S-H

Langmuir			Freundlich		
q_m/(mg·g^{-1})	b /(L·mg^{-1})	R^2	K /(mg·g^{-1})	n	R^2
25.71	0.37	0.99	7.38	2.59	0.77

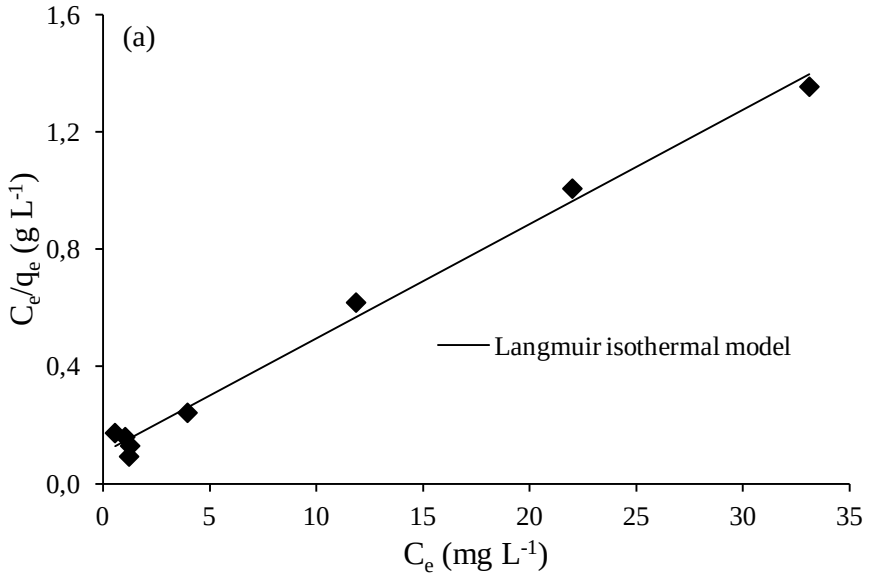

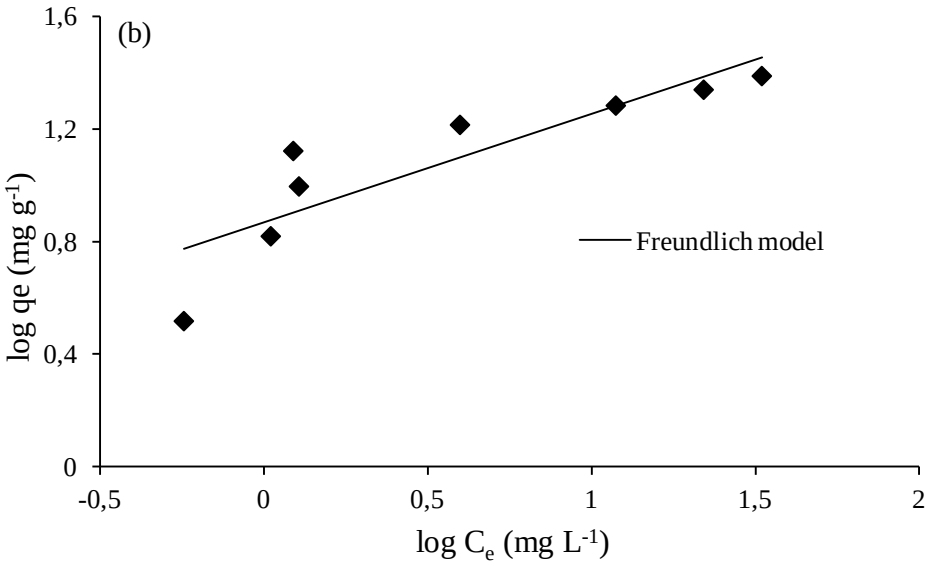

Figure 9 – Isothermal model fitted to experimental data for the uptake of Pb^{2+} (a) Langmuir isothermal model, and (b) Freundlich isothermal model

4.3 Microstructure analysis

FTIR was applied to study the structure variation of C-S-H powder before and after adsorption (Figure 10). In both samples, CO_3^{2-} asymmetric stretching bands due to contamination with CO_2 during samples preparation and drying were detected at 1432 cm^{-1} and 873cm^{-1}. The bending vibration band of molecular H_2O appeared at 1632 cm^{-1}, while the stretching vibration of O-H groups or hydroxyls appeared in the 3433-3440 cm^{-1} region. The most intensive vibration of silicate appeared as a band at the range of 900-1100 cm^{-1} which was attributed to stretching vibration of $[SiO_4]^{4-}$ tetrahedral. The vibration band in C-S-H was at 982 cm^{-1}, however, it shifted to 1075cm^{-1} after adsorbing Pb^{2+}, demonstrating that the polymerisation of silicate chain varied. In addition, the bands corresponding to δ-Si-OH stretching vibration appeared at 1280 cm^{-1} and 756 cm^{-1} in C-S-H, but disappeared after adsorbing Pb^{2+}, suggesting that coordination reaction between Hydroxyl functional group and Pb^{2+} took place as following way:

$$(Si\text{-}OH)+2H_2O+Pb^{2+}=Si\text{-}Pb(OH)_3+2H^+$$

This reaction agrees with the adsorption of Cu^{2+} by asbestos tailings in [29]. It indicates that the presence of active sites in C-S-H structures can cooperate with Pb^{2+} in a relative stable state, which is demonstrated by the desorption results.

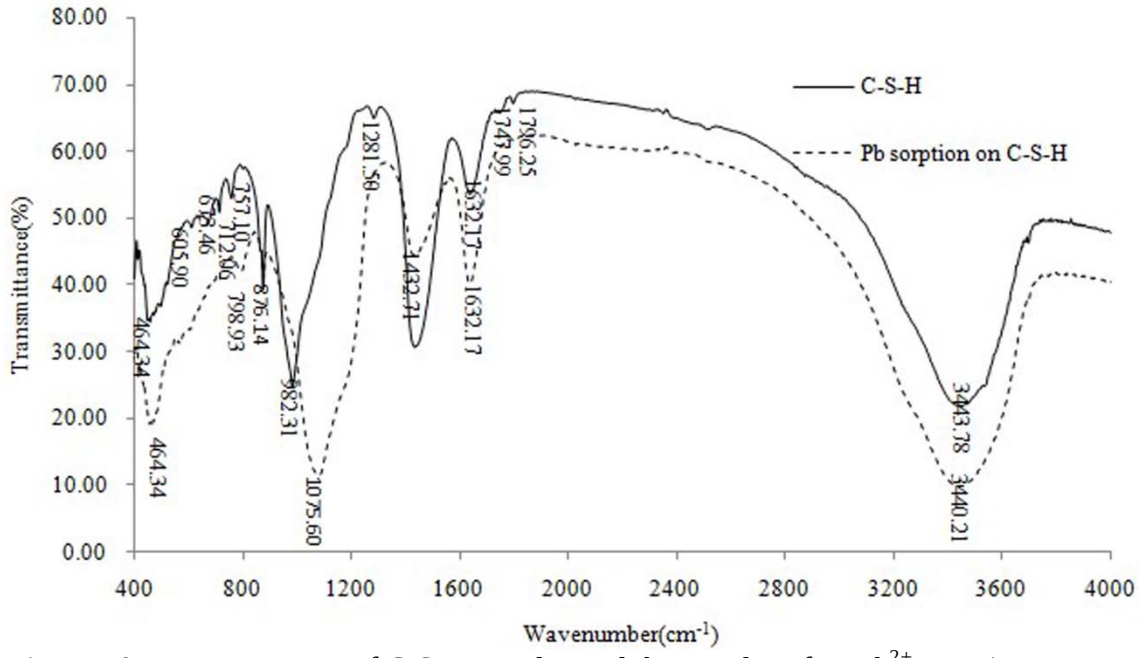

Figure 10 – FTIR spectra of C-S-H powder and the powder after Pb^{2+} sorption

5. CONCLUSION

This study shows that the calcium silicate hydrate synthesized from steel slag is a potential Pb^{2+} adsorbent. The adsorption depends on the Ca/Si molar ratio and lime addition which further affect on the surface properties of powder particles. The most efficient adsorption of the C-S-H has a Ca/Si ratio of 1.5. Pb^{2+} can be effectively removed by this C-S-H powder at the pH value of the solution between 5 and 7. The equilibrium adsorption occurs at 75 minutes when 15 g L^{-1} C-S-H is mixed with 200 mg L^{-1} Pb^{2+} solution. The removal of Pb^{2+} and adsorption capacity is 99.4% and 13.25 mg g^{-1}, respectively. The concentration of Pb^{2+} in the solution after adsorption for more than 120 minutes is lower than 0.5 mg L^{-1}. The low leaching ratio from desorption result indicates that Pb^{2+} can be stably combined by C-S-H.

Kinetic sorption data were in agreement with the Lagergren pseudo-second-order with the equilibrium adsorption of 13.09 mg g^{-1}. In terms of the sorption isotherm, it can be described by the Langmuir adsorption isotherm, the equilibrium adsorption capacity of which is 20.41 mg g^{-1}. The adsorption is controlled by external-particle diffusion stage before equilibrium state, followed by intra-particle diffusion procedure.

ACKNOWLEGEMENT

This work was financed by NSFC (National Natural Science Foundation of China, 50972171) and Graduates Innovation and the Equipmental Administration Faculty of Chongqing University. The Authors also appreciate the support of Chinese Scholarship Council.

REFERENCES

1. Chiang, R.-K. "Calcium-based sorbents for flue gas desulfurization". Case Western Reserve University; 1995.
2. Lai, Y.-L., Thirumavalavan, M.,Lee, J.-F., "Effective adsorption of heavy metal ions (Cu^{2+}, Pb^{2+}, Zn^{2+}) from aqueous solution by immobilization of adsorbents on Ca-alginate beads". *Toxicological & Environmental Chemistry*.Vol. 92,No. 4, 2010, pp. 697-705.
3. Shrivastava, O.P.,Shrivastava, R., "Sr^{2+} uptake and leachability study on cured aluminum-substituted tobermorite–OPC admixtures". *Cement and Concrete Research*.Vol. 31,No. 9, 2001, pp. 1251-1255.
4. Song, Y.L., Wang, Y.P., Song, P.P., et al., "Nonequilibrium thermodynamics study of nuclide migration behavior in the cement based radioactive waste forms". *Journal of Henan University (Natural Science)*.Vol. 36,No. 3, 2006, pp. 21-24.(In Chinese).
5. Zhang, Y.M., Li, X.D.,Sun, W., "Leaching of Copper Wastes Stabilized by Cementitious Material". *Journal of Chinese Ceramic Society* Vol. 30,No. 4, 2002, pp. 536-539.
6. Mehta, P.K.,Monteiro, P.J.K. "Concrete microstructure, properties and materials ". third ed. New York: McGraw-Hill; 2006.
7. Taylor, H.F.W. "Cement Chemistry". London: Thomas Telford; 1997.
8. Chen, J.J. "The nanostructure of calcium silicate hydrate". Northwestern University; 2003.
9. Lan, J.K., Hu, Q.J.,Wang, Y.X., "Adsorption of chromate by calcium silicate hydrate". *Journal of Guilin University of Technology*.Vol. 26,No. 2, 2006, pp. 263-267. (In Chinese).
10. Mandaliev, P., Dähn, R., Tits, J., et al., "EXAFS study of Nd(III) uptake by amorphous calcium silicate hydrates (C–S–H)". *Journal of Colloid and Interface Science*.Vol. 342,No. 1, 2010, pp. 1-7.
11. Pomiès, M.-P., Lequeux, N.,Boch, P., "Speciation of cadmium in cement: Part I. Cd2+ uptake by C-S-H". *Cement and Concrete Research*.Vol. 31,No. 4, 2001, pp. 563-569.
12. Shrivastava, O.P.,Verma, T., "Sr2+ Sorption and leach rate studies on synthetic calcium silicate hydroxy hydrate". *Advanced Cement Based Materials*.Vol. 2,No. 3, 1995, pp. 119-124.
13. Stumm, A., Garbev, K., Beuchle, G., et al., "Incorporation of zinc into calcium silicate hydrates, Part I: formation of C-S-H(I) with C/S=2/3 and its isochemical counterpart gyrolite". *Cement and Concrete Research*.Vol. 35,No. (9), 2005, pp. 1665-1675.
14. Macé, N., Wieland, E., Dähn, R., et al., "EXAFS investigation on U(VI) immobilization in hardened cement paste: influence of experimental conditions on speciation". *Radiochimica Acta*.Vol. 101,No. 6, 2013, pp. 379-389.
15. Li, C.H., "Study on the development and prospect of recycling technology of steel slag in China". *Wisco Technology*.Vol. 38,No. 4, 2010, pp. 51-54. (In Chinese).
16. Wang, S., Peng, X., Tang, L., et al., "Influence of inorganic admixtures on the 11 Å-tobermorite formation prepared from steel slags: XRD and FTIR analysis". *Construction and Building Materials*.Vol. 60, 2014, pp. 42-47.
17. Kuwahara, Y., Tamagawa, S., Fujitani, T., et al., "A novel conversion process for waste slag: synthesis of calcium silicate hydrate from blast furnace slag and its application as a versatile adsorbent for water purification". *Journal of Materials Chemistry A*.Vol. 1,No. 24, 2013, pp. 7199-7210.
18. Han, J.H., Ni, W.,Yu, Y.Z., "Research on treatment of lead-bearing wastewater by xonotlite secondary particles". *Techniques and Equipment for Environmental Pollution Control*.Vol. 7,No. 1, 2006, pp. 22-25.
19. Lee, D., "Formation of leadhillite and calcium lead silicate hydrate (C–Pb–S–H) in the solidification/stabilization of lead contaminants". *Chemosphere*.Vol. 66,No. 9, 2007, pp. 1727-1733.

20. Pierrard, J.-C., Rimbault, J.,Aplincourt, M., "Experimental study and modelling of lead solubility as a function of pH in mixtures of ground waters and cement waters". *Water Research*.Vol. 36,No. 4, 2002, pp. 879-890.
21. Coleman, N.J., Trice, C.J.,Nicholson, J.W., "11 Å tobermorite from cement bypass dust and waste container glass: A feasibility study". *International Journal of Mineral Processing*.Vol. 93,No. 1, 2009, pp. 73-78.
22. Coleman, N.J., Brassington, D.S., Raza, A., et al., "Sorption of Co^{2+} and Sr^{2+} by waste-derived 11 Å tobermorite". *Waste Management*.Vol. 26,No. 3, 2006, pp. 260-267.
23. Liu, S.Y., Ma, S.J., Ye, Z.X., et al., "Absorption kinetics of Pb^{2+} on steel slag". *Environmental Protection of Chemical Industry*.Vol. 27,No. 3, 2007, pp. 214-217.
24. Mandaliev, P., Wieland, E., Dähn, R., et al., "Mechanisms of Nd(III) uptake by 11Å tobermorite and xonotlite". *Applied Geochemistry*.Vol. 25,No. 6, 2010, pp. 763-777.
25. Zhao, X.G., Liu, Z.N.,Wang, G.R., "Preparation of coal fly ash based forming adsorbent and its adsorptive properties for methylene blue". *Journal of Chinese Ceramic Society*.Vol. 37,No. 10, 2009, pp. 1683-1688.
26. Bulut, Y.,Aydın, H., "A kinetics and thermodynamics study of methylene blue adsorption on wheat shells". *Desalination*.Vol. 194,No. 1–3, 2006, pp. 259-267.
27. Wang, S., Xie, L.,Zhou, Q., "Adsorption properties and kinetics of chromium from aqueous solution by steel slag". *China Water & Wastewater*.Vol. 25,No. 3, 2009, pp. 54-57.
28. Zhang, Q.F., Hu, X.F., Jia, X.N., et al., "Study of diffusion equation for describing the adsorbing process of Cr (IV) by peanut shell". *Chemistry and Bioengineering* Vol. 28,No. 2, 2011, pp. 83-85.
29. Zheng, S.L., Zheng, L.M.,Tan, Z.H., "Adsorption of copper ion onto acid leaching residue of asbestos tailings". *Journal of Chinese Ceramic Society*.Vol. 37,No. 10, 2009, pp. 1744-1749.